UNITED NATIONS UNIVERSITY
GEOTHERMAL TRAINING PROGRAMME
Orkustofnun, Grensasvegur 9,
IS-108 Reykjavik, Iceland

Reports 2013
Number 37

# PROCESSING AND 1D INVERSION OF MAGNETOTELLURIC DATA FROM DUBTI AREA IN TENDAHO GEOTHERMAL FIELD, ETHIOPIA

**Behailu Woldesemayet**
Geological Survey of Ethiopia
Geothermal Energy Department
P.O. Box 2302, Addis Ababa
ETHIOPIA
*msemayet@yahoo.com*

## ABSTRACT

Electromagnetic methods are one of the most effective geophysical methods in geothermal exploration. They enable imaging the subsurface conductivity. Magnetotelluric (MT) and transient electromagnetic methods (TEM) are the most successful methods in identifying geothermal resources prior to drilling. The MT method uses the natural source of the electromagnetic field to screen out the resistivity structure down to a depth of several kilometers, whereas TEM uses an artificial source field to image the near-surface resistivity variations down to a depth of around one kilometre. Data collected by these methods are processed. The processed data are used for a 1D Occam inversion to create a resistivity model. This report discusses the processing and inversion of magnetotelluric (MT) data from the Dubti area in Tendaho geothermal field, NE-Ethiopia. TEM soundings from the Krýsuvík area in SW-Iceland are used as an example of the processing and inversion of transient electromagnetic data.

## 1. INTRODUCTION

Geophysical exploration is one of the applied branches of geophysics which includes measurements on the surface, above the surface in the air, and within the earth in boreholes. It measures the physical properties of the earth's subsurface. These physical properties show discontinuities from place to place in a geothermal field. These properties include the propagation of waves, density, magnetic susceptibility, thermal conductivity and electrical conductivity. Geophysical methods are classified into direct methods and indirect or structural methods. Direct methods are thermal and electrical methods. Structural methods are seismics, gravity and magnetics. These methods are helpful in exploring geothermal resources. The electromagnetic methods are especially powerful in exploring geothermal resources. They include a variety of techniques, survey methods applications and interpretation procedures. The electromagnetic methods include the magnetotelluric (MT) and transient electromagnetic (TEM) methods. These methods are used to describe the resistivity structure beneath the surface of the earth. In this report, the main electromagnetic methods, the MT method and the TEM method, are discussed. In addition, 1D modelling of MT data from the Dubti area in Tendaho geothermal field in NE-Ethiopia and the inversion of TEM data from the Krýsuvík geothermal field in SW-Iceland are discussed.

## 2. LITERATURE REVIEW

### 2.1 Geophysical methods for geothermal prospecting

Geophysical methods play a big role in geothermal exploration. They are able to determine what is found beneath the earth's surface, describing the structure of the earth under the surface. The structure of the earth in a certain geothermal field is known through the property of rocks. These properties include the propagation of waves, density, magnetic susceptibility, thermal conductivity and electrical conductivity of rocks which can be measured directly or indirectly. Geophysical methods are classified into, direct and indirect (structural) methods (Hersir and Björnsson, 1991). Direct methods are thermal and electric methods, whereas structural methods are gravity, magnetics and seismic methods. The basic electric methods in modern geothermal exploration, TEM and MT, are discussed in Section 4, and their basis, the electrical resistivity, is discussed in Section 3.

### 2.2 Indirect (structural) methods

Gravity surveys are used to study geological formations through variations of density between subsurface rocks. The density of the rock depends on mineral composition and porosity. This is shown by the Bouguer anomaly. It is used to show geological information that may reveal magmatic bodies, i.e. the heat source. A gravity survey can also be used in groundwater exploration and mineral exploration.

Magnetics are used to measure the variations in the earth's magnetic field. They can be measured using a handheld magnetometer or from the air, that is an aeromagnetic survey. The measurements indicate the variations in the magnetic properties of the subsurface rocks. They may help in mapping faults and dykes.

Seismic waves are pulses of strain energy that propagate in solids and fluids. They are divided into two classes: passive seismic methods and active seismic methods (Lemma, 2007). Active seismic waves are a controlled generation of elastic waves from a seismic source, which can provide an image of the subsurface. Active seismic methods cover all seismic waves having an artificial source, whereas passive seismic methods include natural sources of waves, like an earthquake produced by faulting.

## 3. ELECTRICAL PROPERTIES OF ROCKS

All rock materials have intrinsic properties. One of the intrinsic properties of rocks is its electrical property. The electrical property of rocks can be described by the resistivity. The resistivity of a material is dependent on the geometric parameters and the type of the material it is made of. Consider the conductive material shown in Figure 1. The resistivity, $\rho$ ($\Omega$m), of a material is inversely proportional to its length ($l$) and directly proportional to the cross-sectional area ($A$). Therefore:

$$\rho = R\frac{A}{l} \tag{1}$$

where $R$ = Resistance of the material ($\Omega$);
$l$ = Length of the material (m);
$A$ = Cross-sectional area of the material ($m^2$);
$\rho$ = Resistivity ($\Omega$m).

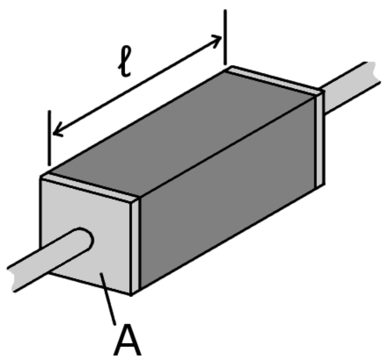


FIGURE 1: A conductive material

According to Ohm's law . electrical resistivity can also be defined as the ratio of the potential difference ΔV to the current I, across a material which has a cross-sectional area of 1 $m^2$ and is 1 m long. This is shown as:

$$\rho = \frac{\Delta V}{I} \tag{2}$$

where $\rho$ = Resistivity (Ωm);
$\Delta V$ = Potential difference (V);
$I$ = Current flow through the material (A).

The electrical conductivity, $\sigma$ (S/m), of the material is the reciprocal of the resistivity, i.e.:

$$\sigma = \frac{1}{\rho} \tag{3}$$

The major conduction mechanisms in rocks are as follows:

- *Pore fluid conduction*: Takes place through ions dissolved in the pore fluid.
- *Surface conduction*: Conduction takes place on the surface of the pores by absorbed ions.
- *Mineral conduction*: Rock matrix creates this type of conduction.

The electrical resistivity of rocks depends mostly on salinity, porosity, temperature, water rock interaction and alteration (Hersir and Árnason, 2009).

### 3.1 Salinity

Conductivity of the pore fluid depends on the salinity and mobility of ions in the solution. The conductivity of a solution, $\sigma$, may be determined by considering the current flow through a cross-sectional area of 1 $m^2$ at a voltage of 1 V/m. This can be described by the equation (Hersir and Björnsson, 1991):

$$\sigma = F\,(c_1 q_1 m_1 + c_2 q_2 m_2 + \cdots). \tag{4}$$

where $F$ = Faraday's number ($9.649 \times 10^4$ C/mole);
$c_i$ = Concentration of ions;
$q_i$ = Valence of ion;
$m_i$ = Mobility of different ions.

Figure 2 shows the relationship between the resistivity of NaCl solutions as a function of salinity at different temperatures. From Figure 2, it is seen that the conductivity of an aqueous solution increases with increasing temperature because of the increase in the mobility of the ions, caused by the lowering of the viscosity of the water. Increasing salinity increases conductivity.

### 3.2 Porosity/permeability

Porosity is the ratio between the pore volume and the total volume of a material. There are three types of porosity: intergranular, joints-fissures and vugular (Hersir and Árnason, 2009). The porosity of a rock can be determined by the equation:

$$\Phi_t = \frac{V_v}{V_T} \tag{5}$$

where $\Phi_t$ = Porosity;
$V_v$ = Volume of void space ($m^3$);
$V_T$ = Total bulk volume of the material ($m^3$).

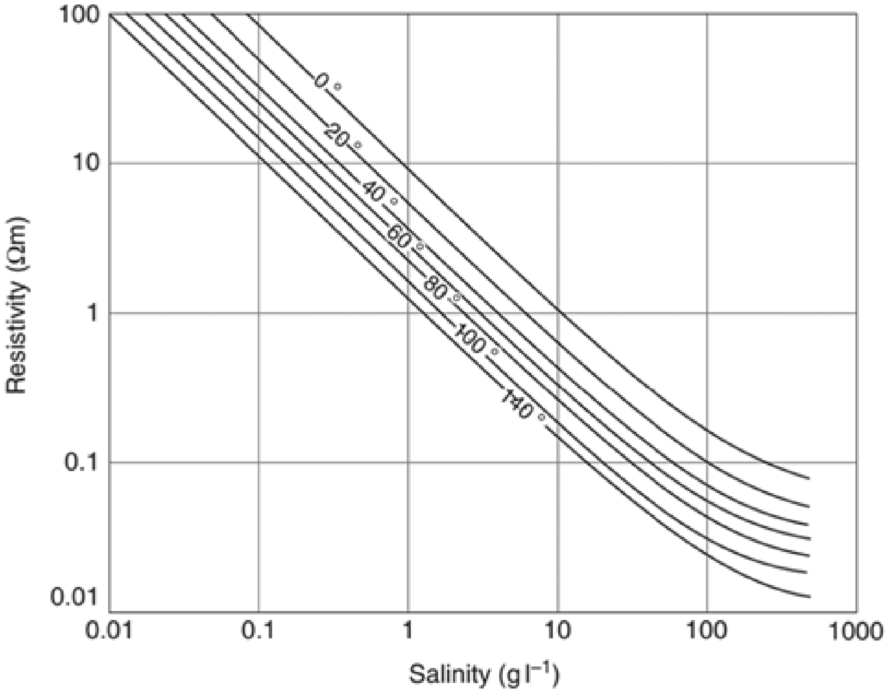


FIGURE 2: The resistivity of solutions of NaCl as a function of concentration and temperature (Flóvenz et al., 2012; based on Keller and Frischknecht, 1966)

The electrical conductivity of rocks is dependent on porosity. The resistivity of water-saturated rocks is related to the porosity according to Archie's law (Archie, 1942) as follows:

$$\rho = \rho_w a \, \Phi_t^{-n} \tag{6}$$

where $\rho$ = Bulk resistivity (Ωm);
$\rho_w$ = Resistivity of the pore fluid (Ωm):
$\Phi_t$ = Porosity;
a and n = Empirical constants.

Archie's law is valid only for pore fluid resistivity, $\rho_w \leq 2$ Ωm (Lemma, 2007).

In some rocks, part of the pore space may be occupied by air (above the water table) or by natural gas, carbon dioxide or petroleum, all of which are insulators. In such cases, Archie's law is modified as follows (Zhdanov and Keller, 1994):

$$\rho = \rho_w a \, \Phi_t^{-n} \quad f^c \tag{7}$$

where $f$ = Fraction of pores containing water of resistivity, $\rho_w$;
$c$ = Empirical constant.

Permeability is the ability of fluids to move within the rock matrix. Permeability depends on the link between pore spaces within the whole rock rather than the porosity of the rock. It is also affected by packing, shape and arrangement of granular materials. Rocks may have high porosity but if the pores are not interconnected then the fluid cannot flow. Therefore, the rock is impermeable even if it has high porosity. The permeability of the rock can be found by the following equation:

$$K = \frac{Q\eta L}{AP} \tag{8}$$

where $K$ = Permeability ($m^2$);
$Q$ = Fluid flow rate ($m^3/s$);

$\eta$ = Fluid viscosity (Pa·s);
$L$ = Length of the rock (m);
$A$ = Cross-sectional area available for flow ($m^2$);
$P$ = Pressure drop (Pa).

### 3.3 Temperature

At moderate temperatures, 0-200°C, resistivity of aqueous solutions decreases with increasing temperature. Temperature has a direct effect on the mobility of ions. Dakhnov (1962) has explained this relationship as:

$$\rho_w = \frac{\rho_{wo}}{1 + \alpha(T - T_o)} \tag{9}$$

where $\rho_{wo}$ = Resistivity of the fluid at temperature $T_o$ (Ωm);
$\alpha$ = Temperature coefficient of resistivity (°$C^{-1}$)
$T$ = Final temperature (°C);
$T_o$ = Reference temperature (°C).

At high temperatures, a decrease in the dielectric permittivity of the water results in a decrease in the number of dissociated ions in the solution. Above 300°C, this starts to increase fluid resistivity.

### 3.4 Interaction of water with rocks (alteration)

Resistivity of rocks decreases due to rock-fluid interaction. The bulk resistivity is decreased by surface conduction along the interface between the rock and water. This can be expressed by Equation 10 (Hersir and Björnsson, 1991):

$$\sigma = \left(\frac{1}{\mathrm{F}}\right)\sigma_w + \sigma_s \tag{10}$$

where $\sigma$ = Bulk conductivity (S/m);
$F$ = Formation factor;
$\sigma_w$ = Conductivity of pore fluid (S/m);
$\sigma_s$ = Interface conductivity (S/m).

If the rocks are fresh and unaltered, then conduction takes place through the pore fluid only. There are relationships between alteration, subsurface resistivity, temperature and the conduction mechanism in high-temperature geothermal systems. Figure 3 shows these relationships for high-temperature geothermal systems in Iceland. The hydrothermal alteration of minerals is affected by hydrothermal water that causes mineral alteration, producing e.g. different clay minerals. The type of minerals formed depends on the temperature and the type of the original rock. Alteration starts at temperatures around 100°C. Below this temperature, there are no altered minerals. In the unaltered zone the conduction mechanism is pore fluid conduction.

There is a change in alteration starting from 100°C. In the range of temperatures from 100 to 250°C, the dominant alteration minerals are smectite-zeolites and mixed-layer clay. Smectites and zeolites exist at temperatures below 200°C, while mixed-layer clays are found between 200 and 250°C. The main conduction in this region is surface conduction in the clay minerals. This zone shows clearly the variation of resistivity with alteration. From 250 to 300°C, mixed-layer clays and chlorite become the dominant alteration minerals. In the high-resistive core (chlorite-epidote), we have surface and pore fluid conduction. Resistivity reflects alteration – in case of fossil system (cooling – alteration temperature is higher than the rock temperature) alteration remains and so does the resistivity structure – the rock temperature is lower than expected. In young systems where the alteration lags behind, the alteration temperature is lower than the rock temperature. And, there are variations in resistivity in both saline and fresh water. Saline water systems are more conductive in all zones than fresh water systems. There is also a change in the conduction mechanism in both systems. At temperatures between 250 and 300°C, conduction mechanisms in salinewater systems are surface conduction in clay minerals, in fresh water systems it is both surface and pore fluid conduction. In other zones, similar conduction mechanisms take place. The original rocks, which consist of minerals, are changed to different types of minerals due to water-rock interaction and chemical transport due to geothermal fluids (Flóvenz et al., 2012). Different zones of mineralization from top to bottom can be seen in Figure 3. The variation of minerals in each zone also has a variation in resistivity because different minerals have different resistivity. In general, the interaction of water with rocks affects the conductivity of the subsurface of a geothermal system.

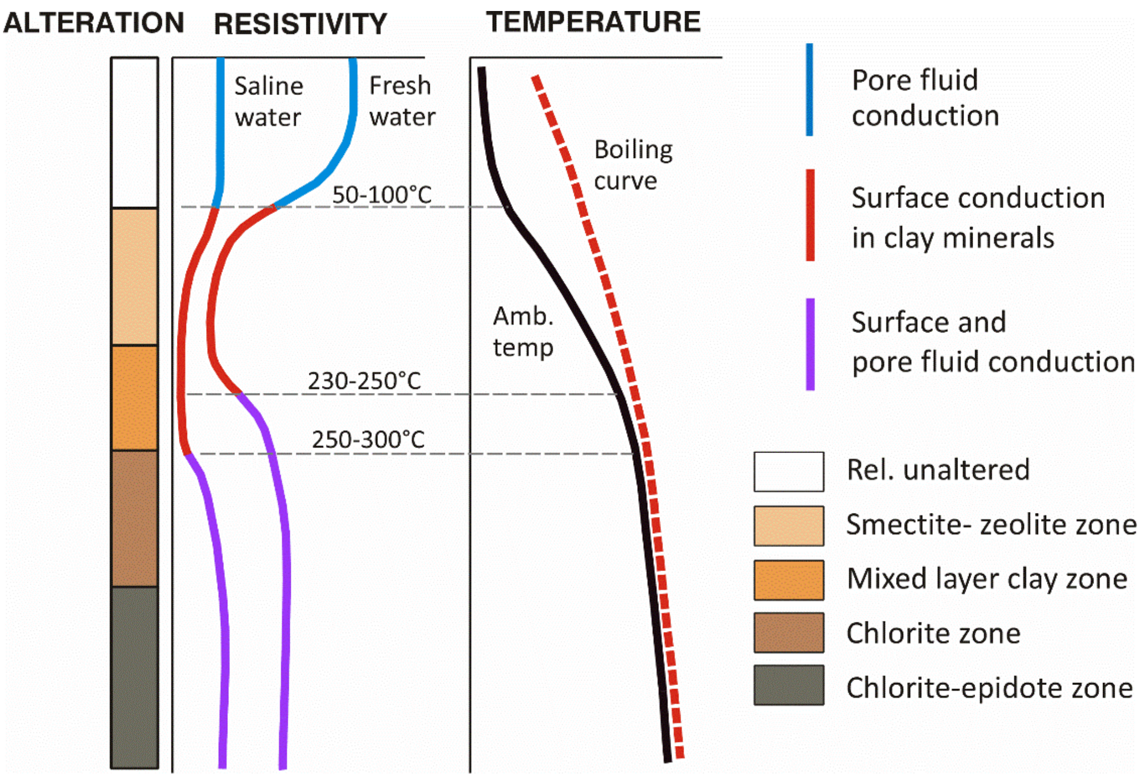


FIGURE 3: General resistivity structure of high-temperature areas in Iceland (Flóvenz et al., 2012; based on Flóvenz et al., 2005)

## 4. THEORY AND SETUP OF MT AND TEM

### 4.1 Theory of TEM

The transient electromagnetic method is a time domain electromagnetic method. It is classified as a grounded dipole or loop source method, depending on how the current from the source is introduced into the ground (Kebede, 2001). Figure 4 shows the central loop method. TEM uses an artificial time-varying magnetic field to induce currents into the earth. A loop of wire is placed on the ground and a constant current is applied to produce a fixed magnetic field. The current is automatically turned off; then the field is decaying in the ground. The decaying field creates a current at great depth. The fluctuation of the decaying magnetic field can be monitored by the receiver coil. The receiver measures the voltage as a function of time. The current distribution and the decay rate of the secondary magnetic field depend on the resistivity structure of the earth. The decay rate as a function of time can be realized in terms of the subsurface resistivity structure (Teklesenbet, 2007). Figure 4 shows a loop of wire placed on the ground, and a constant magnetic field of known value is built up by transmitting a current into the loop.

The depth of penetration of central loop TEM is controlled by how long the induction in the receiver coil can be traced before it is drowned by noise. The induced voltage $V(t,r)$ in the receiving coil in a homogeneous half space of conductivity $\sigma$ is given by (Árnason, 1989):

$$V(t,r) = I_o \frac{C(\sigma\mu r^2)^{3/2}}{10\,\pi^{1/2} t^{5/2}} \tag{11}$$

where $C$ $= A_r n_r A_s n_s \frac{\mu}{2\pi r^3}$;
$A_r$ = Cross-sectional area of the receiver coil ($m^2$);
$n_r$ = Number of turns on the receiver coil;
$A_s$ = Area of transmitting loop;
$n_s$ = Number of turns in the transmitter loop;
$t$ = Time elapsed after the current in the transmitter is turned off (s);
$\mu$ = Magnetic permeability (H/m);
$V(t, r)$ = Transient voltage (V);
$r$ = Radius of the transmitter loop (m);
$I_o$ = Current in the transmitting loop (A).

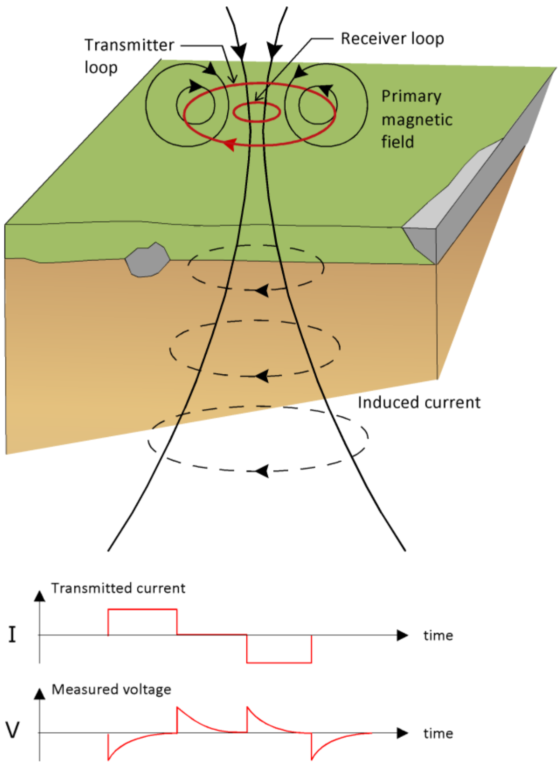


FIGURE 4: TEM sounding setup; the receiver coil is in the center of the transmitter loop; Transmitted current and the measured voltages are shown (Flóvenz et al., 2012)

The result of TEM measurements is calculated as apparent resistivity as a function of time after the current is turned off. The substitution of $\sigma = 1/\rho$ gives the resistivity as:

$$\rho_a = \frac{\mu_o}{4\pi}\left[\frac{2\mu_o I_o A_r n_r A_s n_s}{5t^{\frac{5}{2}} V(t,r)}\right]^{2/3} \tag{12}$$

where $\rho_a$ = Late time apparent resistivity (Ωm).

The curve of the apparent resistivity is inverted to a model with an assumption of homogeneous isotropic layers. The model helps to represent and interpret the data. It leads to a 1D Occam (minimum structure) inversion of the sounding. TEM soundings have better resolution than other artificial source electromagnetic methods because the source loop covers a wide area. However, they are sensitive to other artificial sources of electromagnetic fields such as noise.

## 4.2 Field setup of TEM

TEM instruments are produced by different companies. They have the same function but operate differently. Two of the mostly widely used ones are PROTEM from Geonics, and Zonge from Zonge Engineering and Research Organization. A wire is placed on the ground in a square loop as a transmitter coil. The square loop can be e.g. 200 m × 200 m or 300 m × 300 m. The transmitter coil is connected to the transmitter. Another rectangular loop of size 10 m × 10 m is placed at the centre of the square loop, the receiver loop.

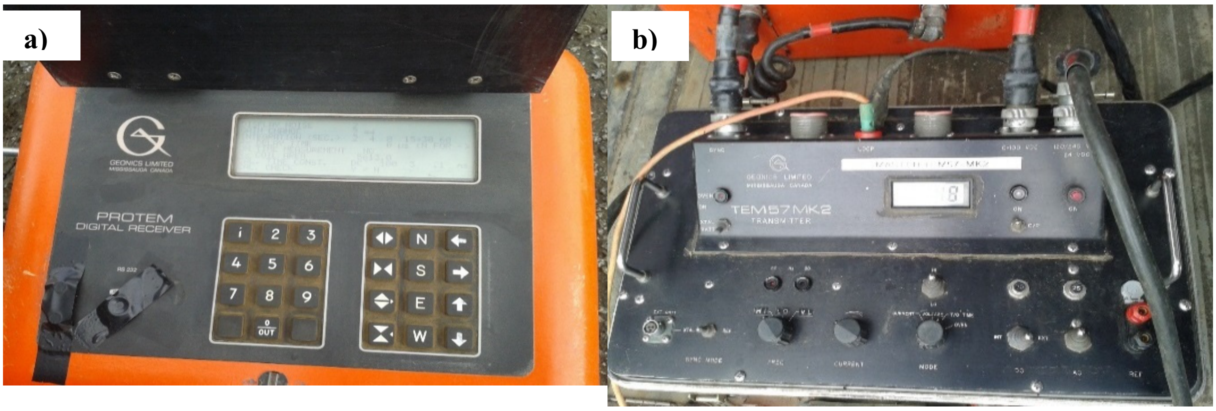


FIGURE 5: TEM equipment: a) Receiver; b) Transmitter

The transmitter and receiver (see Figure 5) are synchronized with crystal clocks so that the receiver knows exactly when the current is ejected through the transmitter loop by the transmitter, which is connected to a signal generator. It produces a magnetic field around the loop. Figure 6 shows the set-up for the TEM method. When the current is turned off automatically, the magnetic field produced by the transmitter loop induces a voltage through the conductive ground. Then the ground again induces a magnetic field in the receiver loop. The magnetic field induced in the secondary coil is vertical in the centre of the transmitter loop. The induced magnetic field produces an electromotive force. The receiver measures this signal as a function of time. The signal is measured at different frequencies by the receiver. At the time when the current through the transmitter is turned off, the current in the ground will be close to the surface, which gives information on the resistivity of the upper layer of the earth. There is always noise in geophysical measurements. Here, there is also noise which comes from lightning and power lines. This noise is reduced by taking repeated measurements.

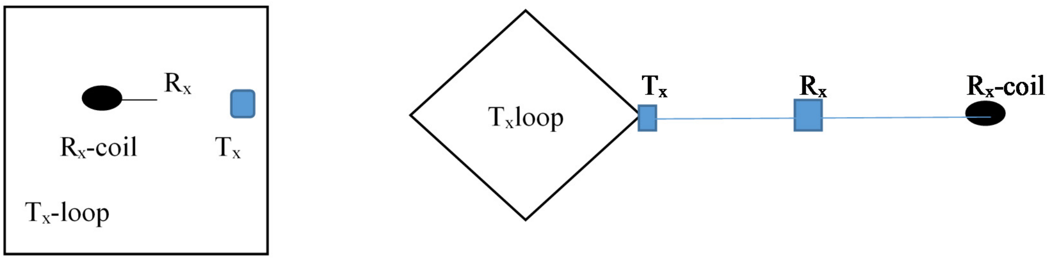


FIGURE 6: Configuration of the TEM method

### 4.3 Theory of MT

The magnetotelluric (MT) method is a passive electromagnetic method. It involves measuring fluctuations in the natural electric **E** and magnetic **B** fields in orthogonal directions on the surface of the earth. It is a means of determining the conductive structure of the earth at depths ranging from a few tens of metres to several hundreds of kilometres (Simpson and Bahr, 2005). There are two sources which give rise to the MT signal (Teklesenbet, 2012):

1. At low frequencies, less than one cycle per second, the source of the signal originates from the interaction of the solar wind with the earth's magnetic field. Solar wind is a stream of charged particles released from the upper atmosphere of the sun. It consists of protons and electrons. They face the earth's magnetic field and are deflected in opposite directions, thereby producing an electric field.
2. Electromagnetic fields which have frequencies higher than 1 Hz originate from meteorological activities, such as lightning discharges. These signals are called sferics.

The behaviour of electromagnetic fields at any period is defined accurately by Maxwell's equations (Simpson and Bahr, 2005). These equations are as follows:

$$\nabla \times \mathbf{E} = -\frac{\partial \mathbf{B}}{\partial t} \tag{13}$$

$$\nabla \times \mathbf{H} = \mathbf{j} + \frac{\partial \mathbf{D}}{\partial t} \tag{14}$$

$$\nabla \cdot \mathbf{B} = 0 \tag{15}$$

$$\nabla \cdot \mathbf{D} = \eta \tag{16}$$

where **E** = Electric field (V/m);
**B** = Magnetic induction (T);
**D** = Electric displacement ($C/m^2$);
**j** = Electric current density owing to free charges ($A/m^2$);
$\eta$ = Electric charge density owing to free charges ($C/m^3$).

The depth of the electromagnetic responses can be estimated by using the electromagnetic skin depth. It is defined as the depth where the electromagnetic field has reduced to $e^{-1}$ of its original real value at the surface (Simpson and Bahr, 2005):

$$\delta(T) = \left(\frac{T}{\pi\mu\sigma}\right)^{\frac{1}{2}} \tag{17}$$

where $\delta(T)$ = Electromagnetic skin depth (m);
$T$ = Period (s);
$\sigma$ = Average conductivity of the medium (S/m);
$\mu$ = Magnetic permeability.

Usually, $\mu$ is assigned its free space value ($\mu_o = 4\pi \times 10^{-7} Hm^{-1}$) and Equation 17 can be approximated as:

$$\delta(T) \approx 500\sqrt{T\rho} \tag{18}$$

where ρ = The apparent resistivity or average resistivity of the medium (Ωm).

Great depths can be screened by the MT method, which is the advantage of this method in comparison to other electromagnetic methods.

The impedance, **Z**, can be defined as:

$$\begin{bmatrix} E_x \\ E_y \end{bmatrix} = \begin{bmatrix} Z_{xx} & Z_{xy} \\ Z_{yx} & Z_{yy} \end{bmatrix} \begin{bmatrix} H_x \\ H_y \end{bmatrix} = \mathbf{Z} \tag{19}$$

This can be realized as the magnetic field being applied to the earth and producing an electric field through electromagnetic induction. The components of the impedance tensor are complex and can be expressed as $Z_{ij}$= Re($Z_{ij}$) + Im($Z_{ij}$) in Cartesian form.

The transfer function in Equation 19 can be minimized into specific expressions, depending on the distribution of electrical conductivity being considered. For a 1D earth, there is no electric field induced parallel to the induced field, and thus, $Z_{xx}$=0 and $Z_{yy}$ = 0 and $Z_{xy}$ = - $Z_{yx}$, or:

$$\begin{bmatrix} E_x \\ E_y \end{bmatrix} = \begin{bmatrix} 0 & Z_{xy} \\ Z_{yx} & 0 \end{bmatrix} \begin{bmatrix} H_x \\ H_y \end{bmatrix} \tag{20}$$

For a 1D earth, the same impedance is measured regardless of the orientation of the *x* and *y* axis.

Apparent resistivity is an average resistivity for the volume of the earth at which a particular period of the electromagnetic field penetrates (Castells, 2006). The apparent resistivity can be derived from the impedance tensor as follows:

$$\rho = \frac{1}{\omega\mu}|Z|^2 = \frac{T}{2\pi\mu}|Z|^2 \tag{21}$$

where $T$ = The period;
$Z$ = Impedance.

Using another system of units, the above equation can also be written as follows:

$$\rho = 0.2T\frac{|E_x|^2}{|H_y|^2} \tag{22}$$

where $\rho$ = Resistivity (Ωm);
$E_x$ = Horizontal electric field (mV/km);
$H_y$ = Orthogonal horizontal magnetic field (gamma);
$T$ = Period (s).

The impedance phase gives additional information about the conductive structure. It can be determined as the tangent inverse of the ratio of the imaginary component of the impedance tensor to the real component of the tensor:

$$\varphi = \tan^{-1}\left[\frac{ImZ}{ReZ}\right]$$

The Tipper is defined as:

$$H_z = T_x H_x + T_y H_y \tag{23}$$

In 1D earth model fields, the Tipper, for the *x* and *y* components, is zero.

For 2D earth, the conductivity is constant in one horizontal direction, but varies in the vertical and the other horizontal direction. The impedance can be rotated mathematically into the strike direction such that the diagonal elements of Equation 19 are both equal to zero, but the off diagonal elements are not the same, i.e.:

$$Z_{xx} = Z_{yy} = 0; \quad \text{and} \quad Z_{xy} \neq Z_{yx}$$

For a 3D earth, the resistivity varies in all three directions. All the impedance tensor elements in Equation 19 are different and the components of the impedances are not equal and non-zero.

### 4.4 Field set-up of MT

The set-up of a MT sounding is shown in Figure 7. It consists of three magnetic coil sensors ($H_x$, $H_y$ and $H_z$), a data logger, four porous pot electrodes, a battery and a GPS antenna. A group of 3 or 4 people can do the field work of an MT survey. Before setting up the survey sites, calibration must be done. There are two things to be calibrated: the instrument and the sensors. This helps in learning the functionality of the instrument and sensors. Calibration of the instrument takes 10-20 minutes. When calibrating the sensors, they are put parallel to each other, 3 m apart. The sensors are connected to the data logger. Then the data logger is started. Recording the data takes 1-2 hours. When the calibration is done, the survey site can be set.

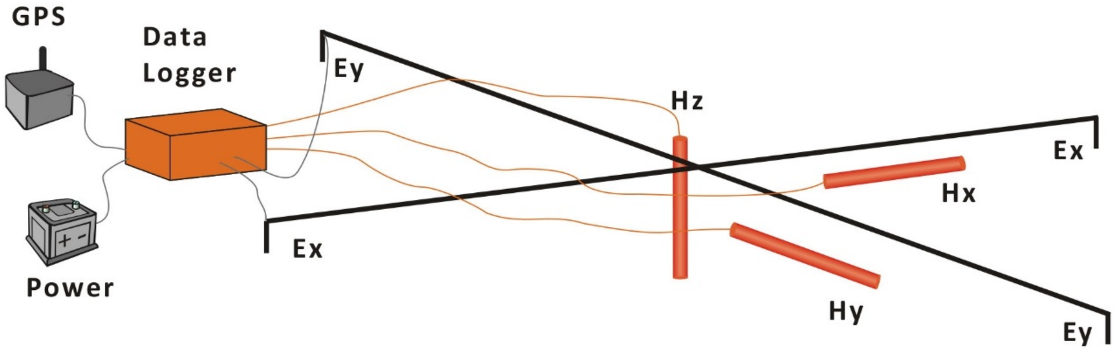


FIGURE 7: Set-up of a magnetotelluric sounding (Flóvenz et al., 2012)

To put up the site, the centre of the site has to be located. Once the site is located, the electrodes and the coil sensors are buried, the electrodes and the sensors are connected to the data logger and the GPS is connected. To do this, the following procedure is followed: First locate the four directions: North, South, East and West using a compass and a tripod. Then align the electrodes towards each direction, 50 m from each if possible. Then dig 30-50 cm for burying the electrodes. Before burying the electrodes, use baked bentonite and put them at the bottom sides of the electrodes to make a good contact with the ground. Figure 8 shows how to bury the electrodes. Four of them are buried in the same way. Then connect the cables to the MTU-5 unit, called the data logger. Besides this, there are three sensor coils which must be buried: one in a North-South direction, the other in an East-West direction, and the third one vertically down. Put the coil some distance from the centre in a north direction, following the path of the electrodes. Align the coil in a N-S direction and make a mark on the ground. Take the coil and bury it in a 40 cm deep horizontal ditch, as shown in Figure 9. Bury the second coil horizontally in an east-west direction; this is checked by using a leveller. Bury the third coil vertically in a 1.5 m hole. Connect the cables which extend from the coils to the unit. Finally, the GPS is connected to the unit.

FIGURE 8: Buried MT electrode

FIGURE 9: Arrangement of an MT coil

The unit is powered by switching a red button to on and releasing it. The LED indicator between the North and South E-line terminals blinks at first and, after a slight delay, it will light steadily. After around 30 seconds, the unit starts up and begins finding satellites. It blinks four times when it has acquired at least four satellites. It also registers the electric dipole length, pot resistance, potential difference and the alignment of the coils. Then it starts to record the data. It is compulsary to stay until it finishes all these things. The data logger is left as it is, with a plastic cover for safety. Data are continuously recorded on a flash card inside the unit until the next day. After checking if the unit recorded data, it is switched off by the user. The flash card is removed from the unit and connected to the computer. Then data are copied to the computer and are ready for processing using SSMT2000 software.

## 5. PROCESSING AND 1D INVERSION OF TEM SOUNDINGS

### 5.1 Processing of TEM soundings

Processing of TEM soundings here requires the use of a UNIX computer operating system. It is a multipurpose operating system which has many users. In this system, there is software called TemX (Árnason, 2006a). TemX downloads data. It operates the voltage data as a function of time after the current turn off with respect to the current in the transmitter. Moreover, it also considers the area covered by the antenna and the gain. Those parameters are displayed on the screen of the receiver, graphically and analytically. This helps the user to remove the outliers and calculate the mean value of the data. It also evaluates the apparent resistivity. A PROTEM receiver is used to retrieve the data. The raw data files are called: .fru. They are extracted by TemX. When data are recorded by the receiver, there may be errors made by the crystal clocks. In addition to this, there may be missing data of the turn off time. These two things can be corrected for when opening the raw data. Data are represented in a graphical form as shown in Figure 10. There are two plots on the screen. On the right is resistivity versus logarithmic time, and on the left, voltages multiplied by $t^{5/2}$ vs. logarithmic time. On both graphs there

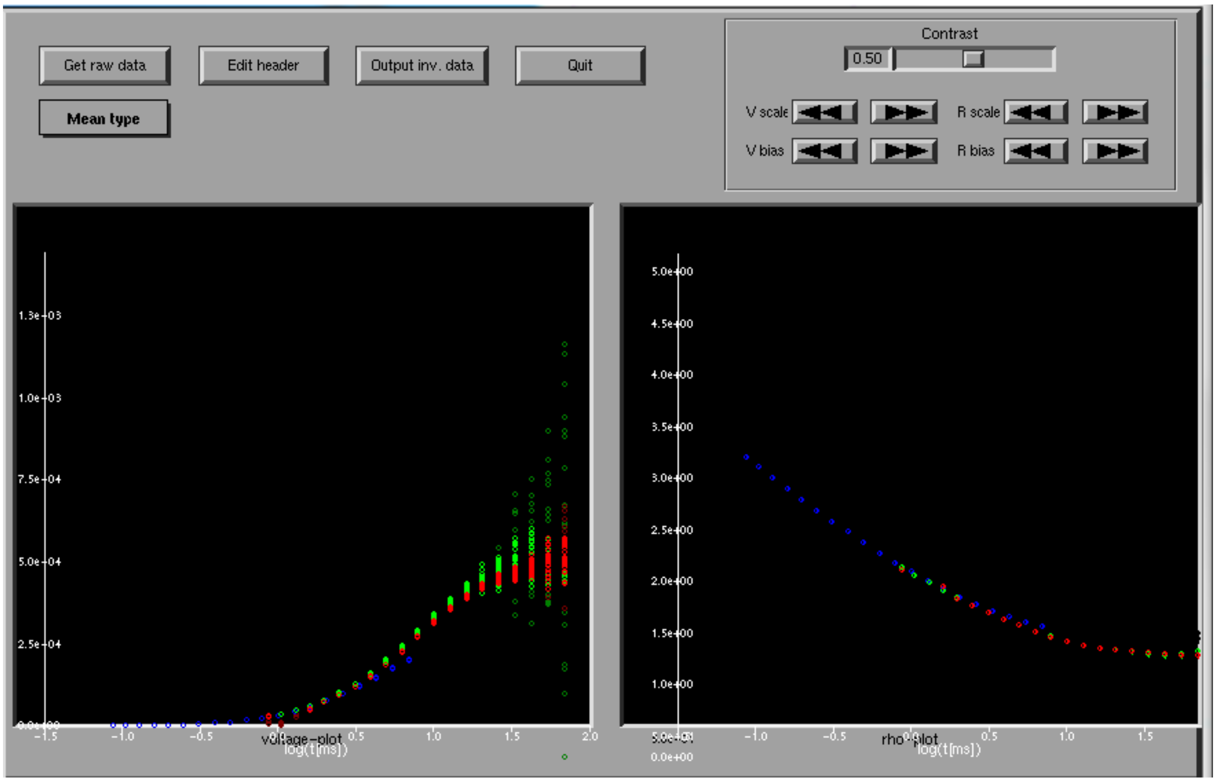


FIGURE 10: Edited raw data from a TEM sounding

are three colored curves. The blue curve is for high-frequency data from the small receiver loop. The green one is for high-frequency data from the small receiver loop and the red curve is for low-frequency data from the big receiver loop. There are points which deviate from the relatively smooth graph line (outliers); these points are edited or masked. Once this editing work is done, click on the edit header to edit the UTM coordinates, the area where the sounding was done, etc. Then click on quit. This saves what was edited. Click on the output .inv file and save the output data of this sounding. Then this sounding is ready for inversion in the TEMTD program.

### 5.2 1D inversion of TEM soundings

The inversion of TEM soundings involves a software called TEMTD which works in a UNIX environment (Árnason, 2006b). Data are prepared in TemX and fed into TEMTD using a script with an initial model. Once the model inversion is produced, that model is used in the Occam inversion to produce the final model. Figure 11 shows the resistivity vs. depth of TEM 1D Occam (minimum structure) inversion. These data are from the Krýsuvík area in SW-Iceland. The area is one of the high-temperature geothermal fields in SW-Iceland. Different parameters can be changed in the script to get a smoother curve. On top of Figure 11, there are two numbers: TEM443962 is the name of the sounding; the other number is the misfit function, i.e. the difference between the measured data and the calculated data. The misfit value should be as low as possible so that the measured and the calculated data are close to each other. Here the value is 0.366.

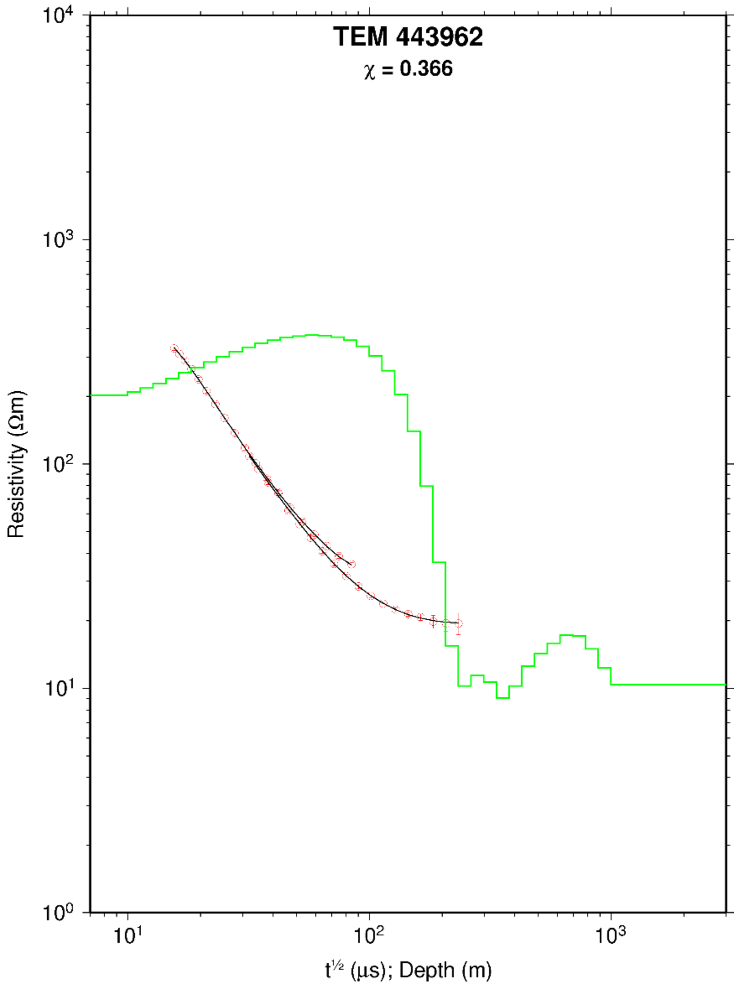


FIGURE 11: 1D inversion of a TEM sounding from the Krýsuvík area, SW-Iceland; Red circles: measured late-time apparent resistivity (different datasets for different receiver loop sizes and current frequencies); black line: apparent resistivity calculated from the model shown in green; Below the name of the TEM station (TEM 443962) at the top of the figure is the misfit function, the root-mean square difference between the measured and calculated values ($\chi$=0.366)

## 6. PROCESSING AND 1D INVERSION OF MT SOUNDINGS FROM THE DUBTI AREA IN TENDAHO

### 6.1 Processing MT soundings from the Dubti area

Tendaho geothermal field is one of sixteen geothermal fields found in the Ethiopian rift. It is located in the northeast part of Ethiopia in the Afar Regional State, in Dubti Wereda. Potential sites of Tendaho geothermal field are Ayrobera, Dubti and Alallobad. Ayrobera and Alallobad are in the surface exploration stage. Much work has been done in the Dubti area. Figure 12 shows the location of Tendaho geothermal field. The Dubti shallow geothermal resource is located at about 600 km distance northeast of Addis Ababa, and is found in the northwest part of the Tendaho Graben, central Afar depression. The nearest town in the project area is Semera, which is the recent capital city of Afar. Tendaho Graben is transsected by an excellent tarmac highway that serves as the main transport route for Ethiopian's foreign trade through Djibouti. Accessibility to the project area is very good. It is possible to reach the area from Addis Ababa along two main highways: the Addis Ababa – Nazareth – Awash – Semera and Addis Ababa – Kombolcha – Semera routes. These are mainly asphalt roads and partly weathered road, shown by a green line in Figure 12. This area is mainly covered with vegetation that is common with arid climatic conditions. The geologic outline of this area is unique because of its location at the juncture of three major rifts: the main Ethiopian rift, the Red sea and the Gulf of Aden rift. It is a place where continental drift takes place. Repeated tectonic activity, volcanism and sedimentation accompanied by tectonics, erosion and eoline activities made their own contributions to the present structure of the area. This low lying flat land is formed mainly by Fluvo-lacustrine and eoline sediment and recent central fissure axial volcanics. Asphalt roads that can be used within the study area are the Semera – Aysiata, Semera – Dobi and Semera – Logiya roads for the Dubti & Ayrobera surface manifestations and the Logiya fossil hydrothermal deposit, respectively. Access within the Dubti surface manifestation area is possible along an abandoned state farm road (Dubti Cotton plantation shown in red box in Figure 12). One can drive on plain land to reach Ayrobera after turning away from the Semera-Dobi asphalt road (~17 km from Semera), although sandy ground makes accessibility more difficult. A local guide is necessary to avoid the sandy ground. There are numerous foot trails in the study area (the entire plain land that dominates the study area can be used as a foot trail, see Figure 13).

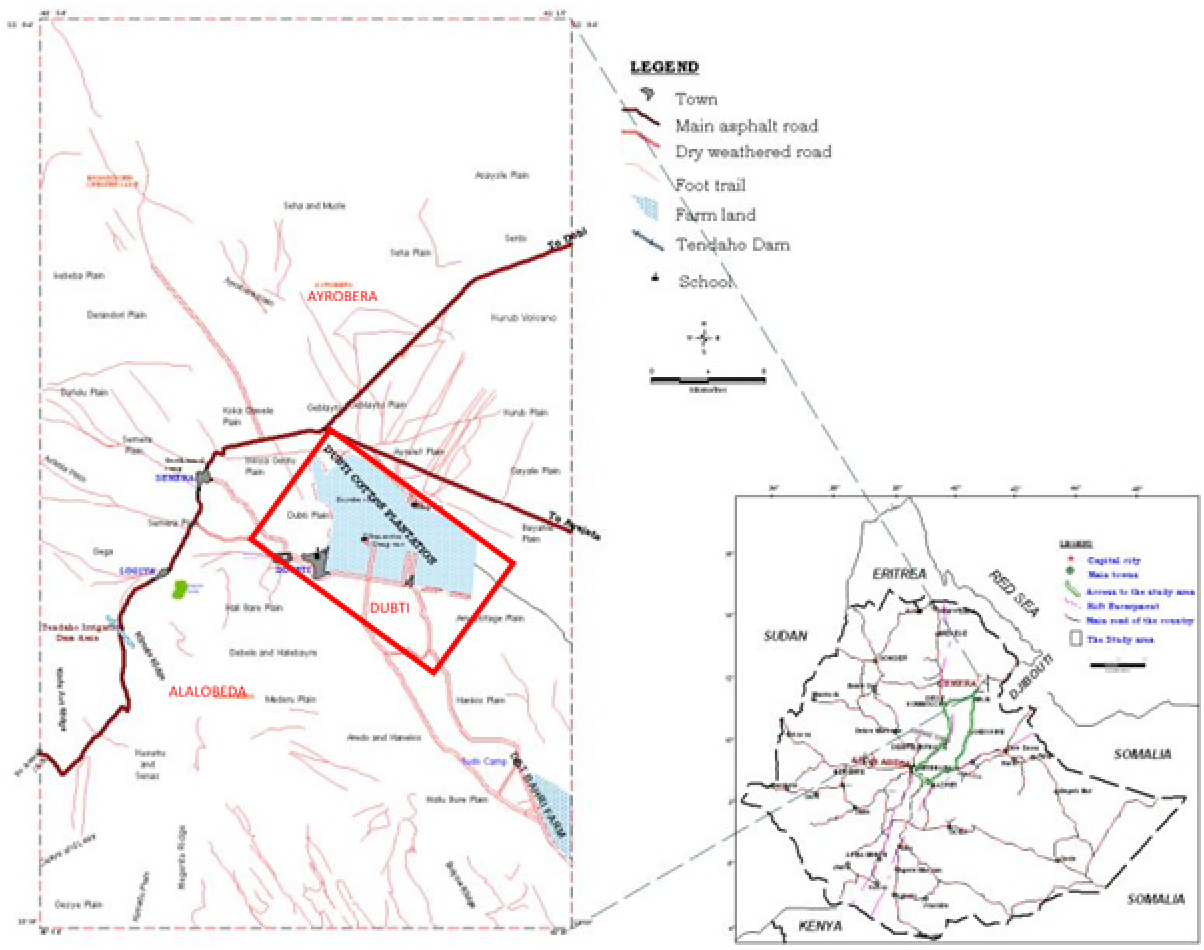


FIGURE 12: Location of the Tendaho Dubti geothermal field
(Megersa and Getaneh, 2006)

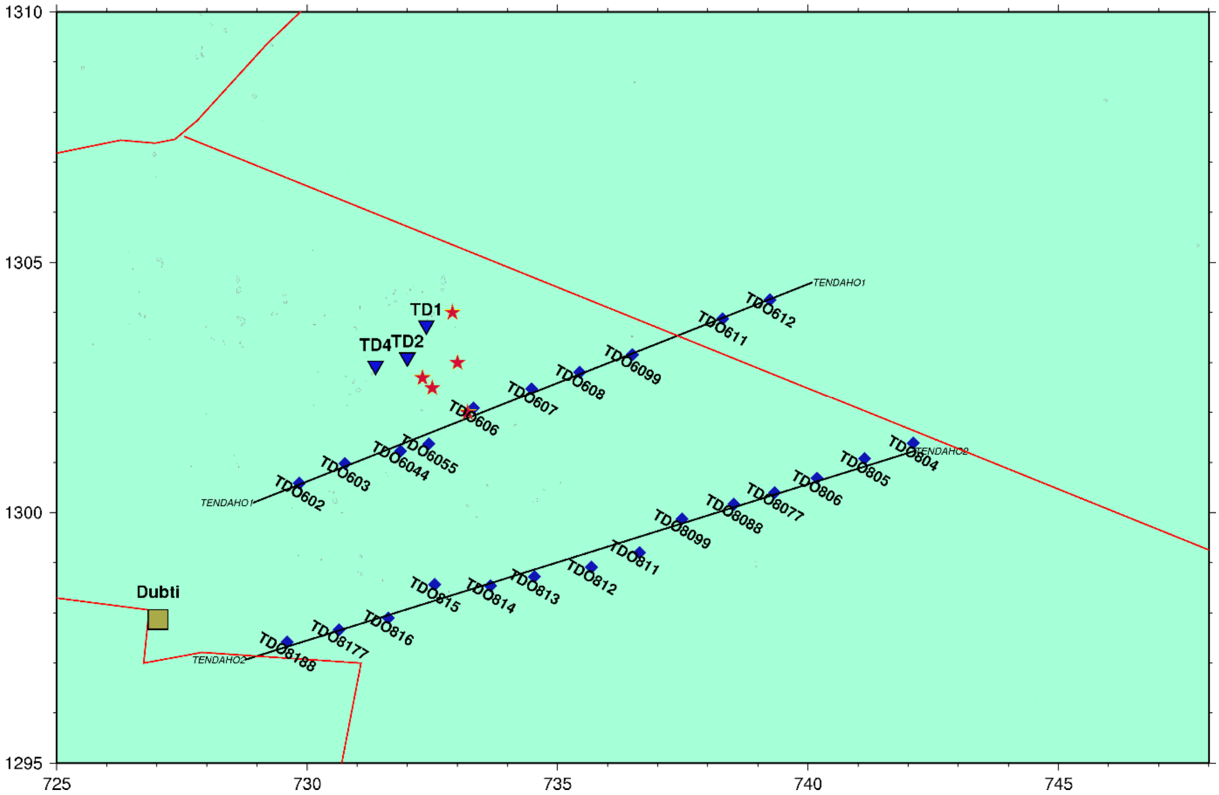


FIGURE 13: Location of MT soundings in the Dubti area (UTM37, datum: ADINDAN Ethiopia, in km); blue diamonds denote MT soundings, red stars are fumaroles, and blue triangles are wells; red lines are roads

### 6.1.1 Review of previous work

The first reconnaissance survey was done by UNEP-EIGS in 1973 (Megersa and Getaneh, 2006). The survey indicated the existence of geothermal resources. Following the recommendations given by the survey and other studies, an agreement was reached between the Ethiopian and Italian governments to try and locate the resources in the Tendaho area. In the first phase geologic, hydrogeology, geochemistry and preliminary geophysics studies were carried out in 1979. The second phase continued in 1980 by including geophysics and drilling of shallow temperature boreholes. The aim of these studies was discovering economically exploitable reservoirs. The results of the study showed significant geothermal resources.

With capital from the Italian government, exploration drilling was carried out between 1993 and 1995. Three deep wells (TD1-TD3) were drilled to a depth of 1.5 to 2 km and one shallow well (TD4) to a depth of 0.5 km. The Geological Survey of Ethiopia drilled additionally two shallow wells (TD5 and TD6). The results of the deep drilling showed a high temperature of 200-270°C. The reservoir is liquid-dominated and shallow, characterized by low-salinity non-condensable gasses. Out of the six wells, four of them could supply enough steam to operate a pilot power plant of 5 MWe.

### 6.1.2 MT survey

MT surveys were carried out to further delineate the resource. The MT surveys were conducted in 2010-2013. The surveys conducted in 2013 in the Dubti area were done by the Geological Survey of Ethiopia. More than 80 soundings were done in Tendaho geothermal field that year. Among these are 30 soundings on two profiles from the Dubti area. The area is covered by a sugarcane plantation. The soundings were done in this plantation. Figure 13 shows the location of the soundings with the two profiles.

The instruments used for MT data collection were two Phoenix units. The system has the following components:

- Five channel MTU-5 unit (data logger);
- Coil sensors;
- Porous pot electrodes of dipole length 100 m;
- Batteries of 12 V;
- GPS tripod;
- Extra cables.

The components are connected in a site as discussed in the setup of MT method in Figure 7. Data are recorded and saved on a flash card which is placed in the data logger. On the next day, the flash card is taken out of the unit and connected to the computer to transfer data to the computer, to process and store. Once the data are transferred to the data logger, the data on the flash card are erased to make it ready for the next station. Raw time series data were recorded in the Dubti area in the Tendaho geothermal field. A total of 24 soundings were carried out in the field. The time series data were downloaded into a program called SSMT2000 from Phoenix.

### 6.1.3 Data processing

The first step of MT data processing involves Fourier transformation from the time domain to the frequency domain. To do a Fourier tramsform, Window-based software called SSMT2000 was used. It takes raw time series data, calibration files and site parameter files as inputs. All sites to be processed have identical frequency parameters. Soundings which have to be processed are selected. The calibration files are also selected together with the site parameter file. Click the TS to FT button on or select from the processing menu. Then the program starts to transform the time series to Fourier coefficients. In robust processing, the auto- and cross-powers are calculated. Finally, these are edited in the Phoenix programme MTEditor, masking outliers. The product is exported as edi-files (SEG, 1991), later to be used as an input to the TEMTD program.

## 6.2 1D Occam inversion of MT soundings

TEMTD is a program which inverts MT and TEM data alone or it inverts jointly MT and TEM data (Árnason, 2006b). Here, it was used for the inversion of MT data. First, data are converted for access in a UNIX operating system, applying the script dos2unix. This makes the files ready to run in the UNIX environment. Then spect2edi is applied to transform the data into .EDI form. The .EDI files are fed into the TEMTD programme. Initially, a model file should be produced. Then, using the model file, an Occam inversion is run using scripts in Unix. To achieve a good fit, some parameters can be changed or improved according to the fit. It is also possible to vary the number of layers to get a good fit. Furthermore, many more iterations can be used in order to get a good fit. Figure 14 shows the 1D Occam inversion of one sounding. It shows apparent resistivity versus period, phase versus period and depth versus resistivity. The depth is estimated to be 30 km.

### 6.2.1 Static shift

Static shift is caused by near-surface resistivity inhomogeneities close to the electric dipoles. It is common in geothermal fields in volcanic areas. There are two things that produce static shifts. These are: voltage distortion (dependence of the electric field on the resistivity where the voltage is measured); and current distortion or current channeling (Árnason, 2008). These two phenomena scale the magnitude of the electric field at the surface by a certain unknown factor. It has no effect on the phase of the electric field. The scale of the electric field also affects the measured apparent resistivity in volcanic geothermal systems. In sedimentary areas like Tendaho geothermal field, static shift has until now not been regarded as a problem because near the surface and at shallow depth the geology of the area is sedimentary deposits and sedimentary formations. Moreover, previous data show that there is little shift in the magnitude of the apparent resistivity. The scaling of the magnitude of the electric field (resistivity) is almost one. The solution to this phenomenon is doing joint inversion of MT and TEM data. Since inhomogeneities are at shallow depth, joint inversion helps to resolve the shift factor (Árnason, 2008).

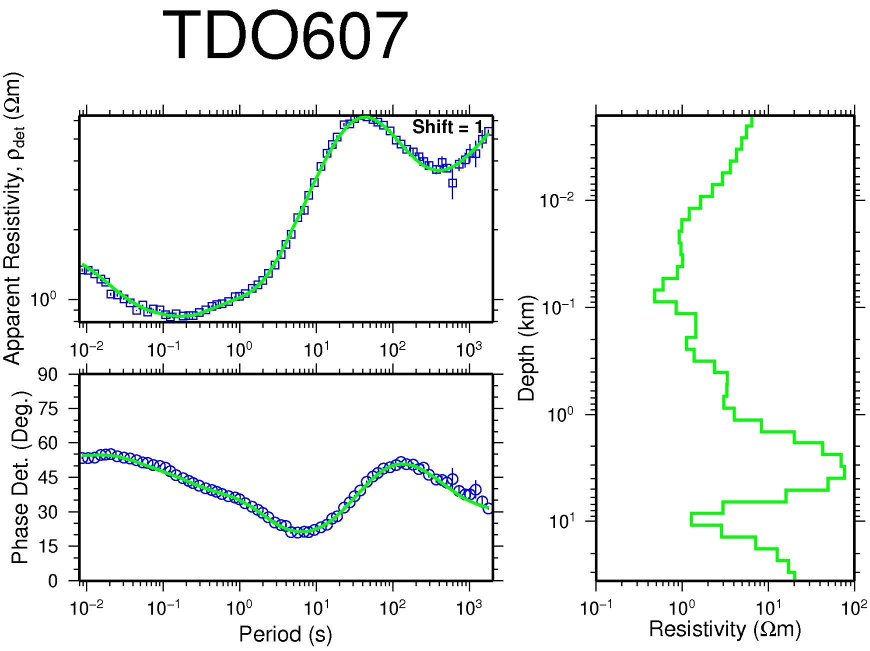


FIGURE 14: 1D Occam inversion of an MT sounding; blue squares: measured apparent resistivity; blue circles: apparent phase – both derived from the determinant of the MT impedance tensor; green lines: on the right, results of the 1D resistivity inversion model, to the left its synthetic MT apparent resistivity and phase response

## 7. INTERPRETATION OF THE INVERSION

### 7.1 Cross-sections

Figure 13 shows the location of two MT cross-sections which run from southwest to northeast. The two cross-sections are parallel, 1 km apart. To plot the results of the inversion, the scripts TEMCROSS and TEMRESD were used (Eysteinsson, 1998). These programs run in a UNIX environment.

Figure 15 shows cross-section Tendaho 1, which runs from southwest to northeast. It is characterized by a low-resistivity anomaly of < 1 Ωm, reaching from the surface down to a depth of around 300 m b.s.l. At a depth of 1.9 km, the resistivity has become quite high. Below sounding TDO606, there is higher resistivity near the surface than below the neighbouring soundings. This is probably due to static shift or three dimensional variations of the resistivity. There is a well between MT sounding TDO605 and TDO606. This is well TD2, directionally drilled. The depth of the well is 2100 m and it is productive. The kick off point of the well is at 885 m. The formation temperature of the well increases from the surface down to a depth of 650 m (Amdeberhan, 1998), as shown in Figure 15. Near the surface, the temperature is 100°C. Then, at a depth of 160 m, the temperature is 200°C, and at a depth of 380 m it is 240°C. In the cross-section, this depth shows a low-resistivity anomaly. This is presumably related to the smectite–zeolite zone. There is a high-resistivity layer below the low resistivity. This high-resistivity anomaly is most likely the chlorite-epidote zone. Figure 16 shows cross-section Tendaho 1 down to a depth of 10,000 m. Below the high resistivity layer, there is a low-resistivity zone at a depth of 6000 m b.s.l. The high resistivity extends through the low resistivity below MT sounding TDO606. This could be due, as mentioned earlier, to static shift. Therefore, it is necessary to do TEM in that area to correct for the shift.

Figure 17 shows cross-section Tendaho 2 down to a depth of 2500 m, which runs parallel to cross-section Tendaho 1. It includes 13 soundings. There is a low-resistivity anomaly < 0.7 Ωm from the

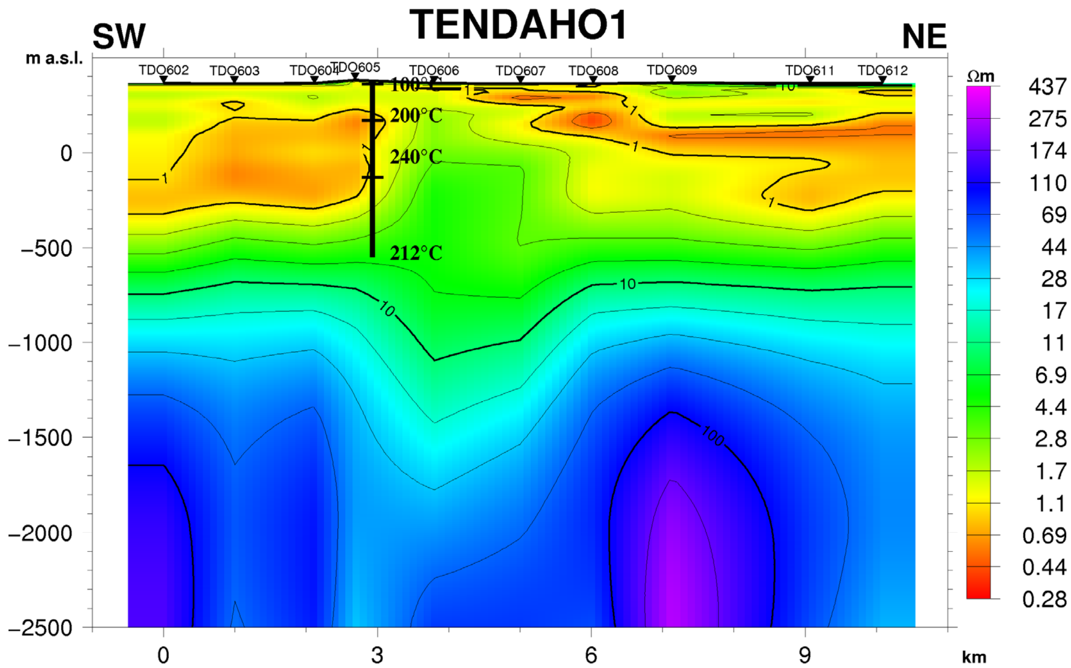


FIGURE 15: MT resistivity cross-section Tendaho 1 down to a depth of 2500 m; for location see Figure 13

surface down to a depth of 800 m. Below MT sounding TDO807, there is a zone of higher resistivity than in the neighbouring soundings. This could be due to static shift of the area or three dimensional variations of the resistivity. The low resistivity near the surface is presumably the smectite-zeolite hydrothermal alteration zone. Below the low-resistivity anomaly there is a high-resistivity zone, clearly seen in Figure 18, which shows the cross-section of Tendaho 2 down to a depth of 10,000 m. High resistivity starts at a depth of 1000 m and extends to 4000 m b.s.l. This high-resistivity zone is most likely the chlorite-epidote zone. Below the high-resistivity zone there is a low resistivity < 1.1 Ωm, probably connected to the heat source.

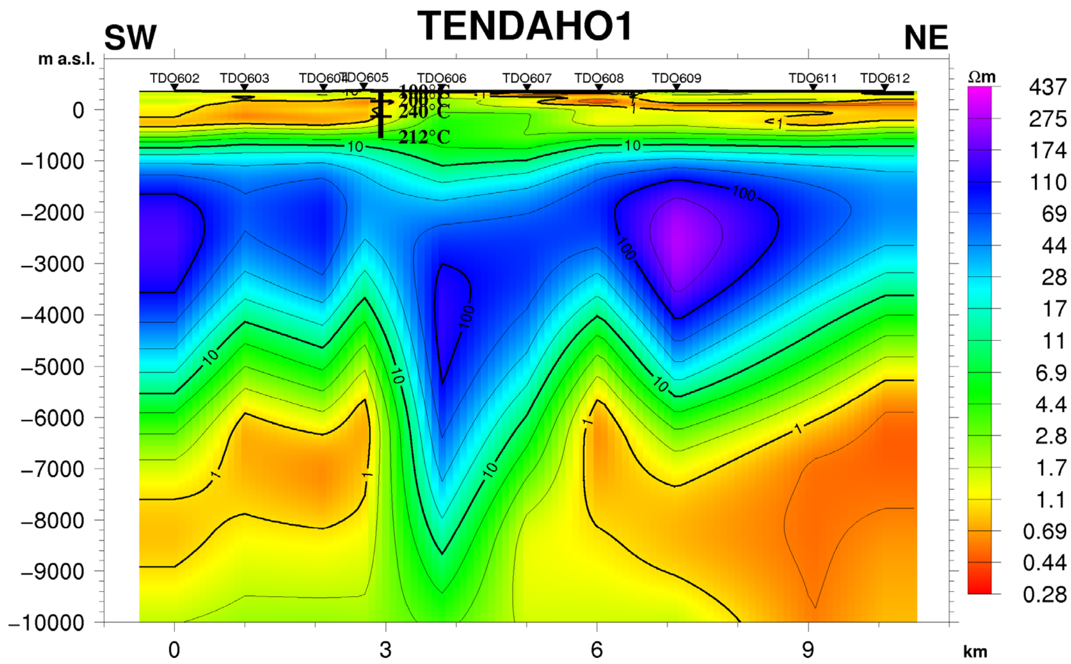


FIGURE 16: MT resistivity cross-section Tendaho 1 down to a depth of 10 km; for location see Figure 13

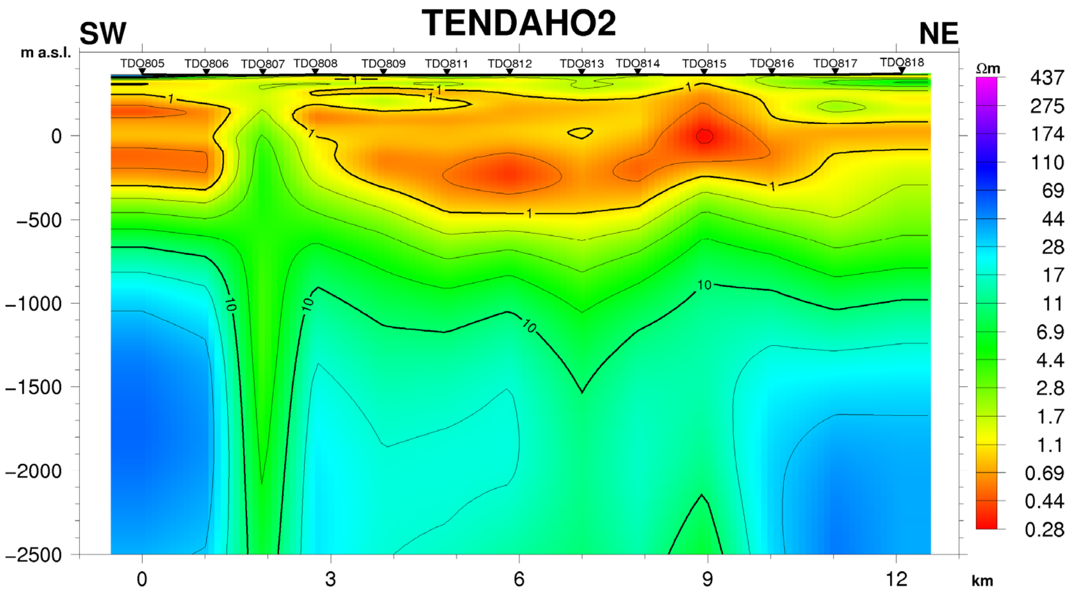


FIGURE 17: MT resistivity cross-section Tendaho 2 down to a depth of 2500 m; for location see Figure 13

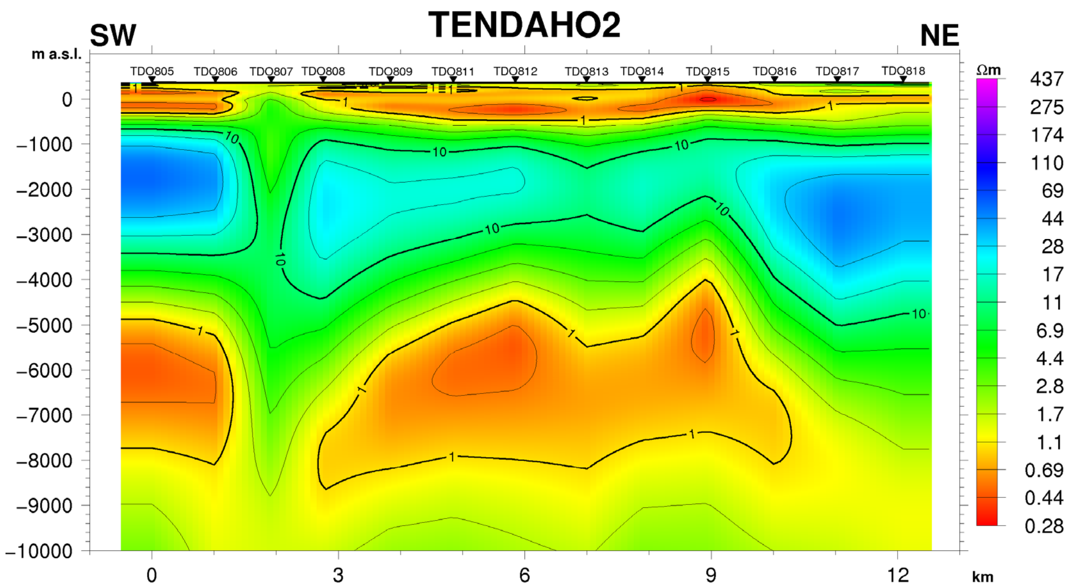


FIGURE 18: MT resistivity cross-section Tendaho 2 down to a depth of 10 km; for location see Figure 13

These resistivity cross-sections can be related to the geological stratigraphy of the wells. Figure 19 shows the borehole geological stratigraphy of wells TD2, TD4 and TD1. From the surface down to a depth of 1100 m, it is composed of sediments, both fine and coarse. There are also recent basalts in this zone. Below 1200 m, the geological structure is made up of the Afar Stratoid basalts.

### 7.2 Iso-resistivity maps

An iso-resistivity map shows the lateral resistivity variations at a certain depth below the surface. Figure 20 shows resistivity variations at sea level. The resistivity is a bit higher near the surface manifestations. In general, the map shows low resistivity. This is seen clearly on the cross-section, as well, showing low resistivity at this depth, which correlates to the smectite-zeolite zone.

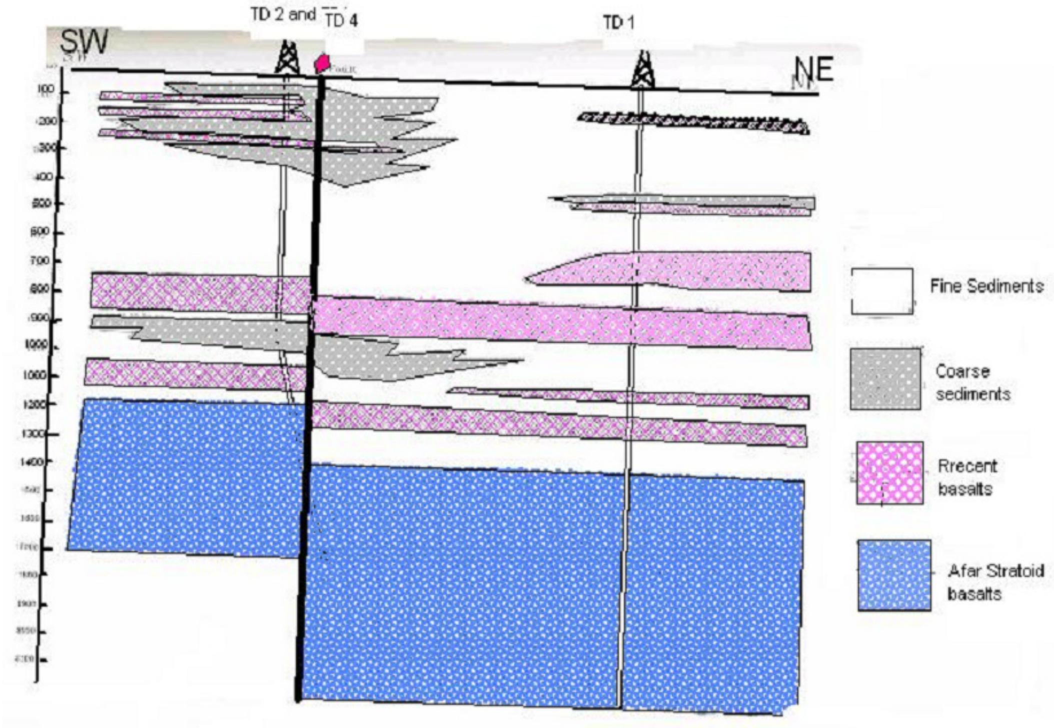


FIGURE 19: Geological stratigraphy of wells TD2, TD4 and TD1
(for location see Figure 13)

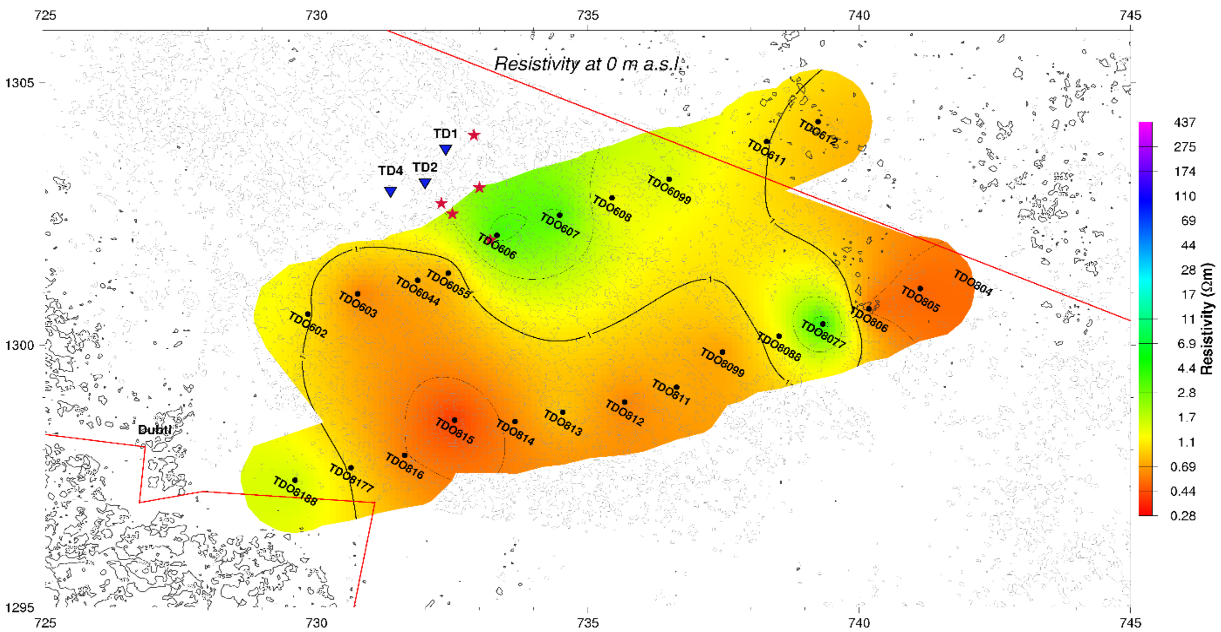


FIGURE 20: Iso-resistivity map at sea level; black dots denote MT soundings,
red stars are fumaroles and blue triangles are wells; red lines are roads

Figure 21 shows the resistivity at 2500 m below sea level. Here, there is a higher resistivity, which can also be seen in profiles Tendaho 1 and Tendaho 2. This section of the map fits with both cross-sections at this depth. The resistivity is related to the chlorite-epidote alteration zone.

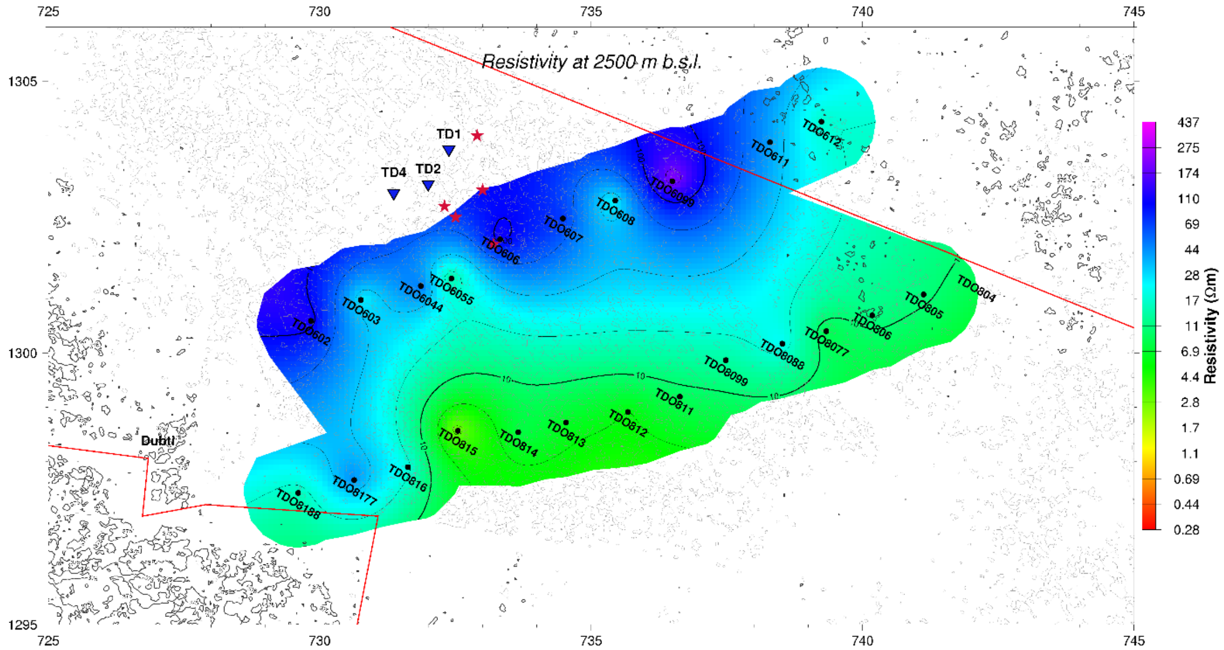


FIGURE 21: Iso-resistivity map at 2500 m b.s.l., for legend, see Figure 20

The third iso-resistivity map was taken at a depth of 6500 m below sea level (Figure 22). It shows low resistivity as on the cross-sections except near sounding TDO606. Here, there is a little higher resistivity than for the rest of the area. It is near the fumaroles. It could fit a heat source or a fracture zone.

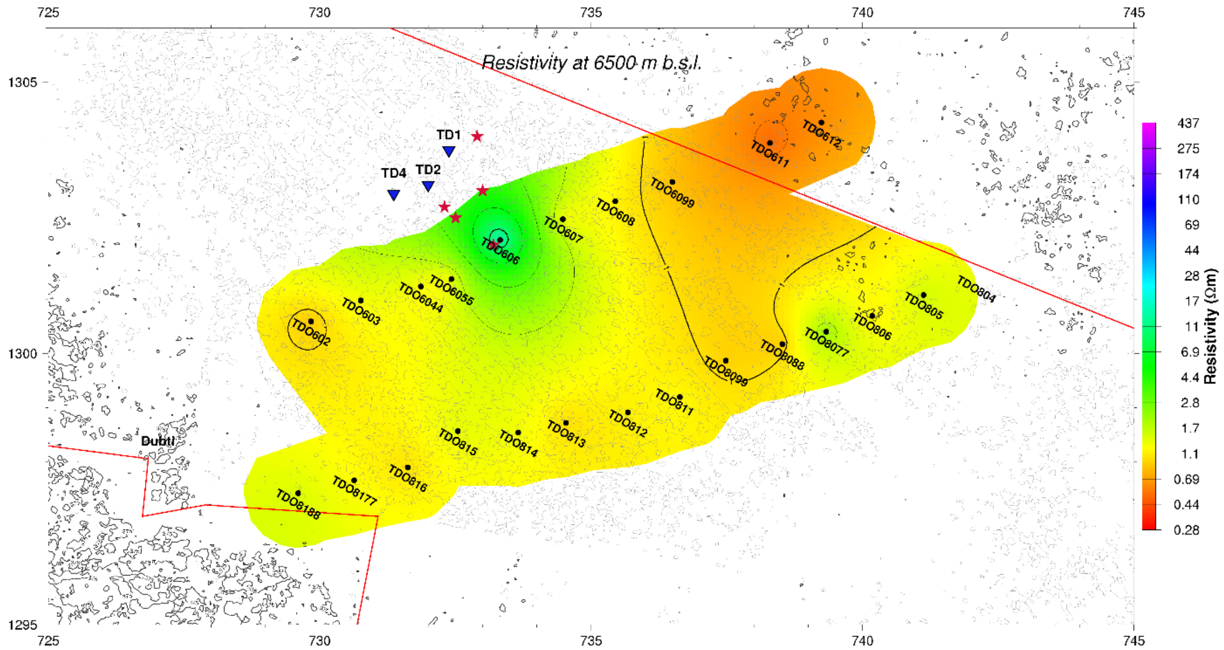


FIGURE 22: Iso-depth resistivity map at 6500 m b.s.l., for legend, see Figure 20

## 8. CONCLUSIONS AND RECOMMENDATIONS

Cross-sections Tendaho 1 and Tendaho 2 show the same features. They show similar resistivity values at similar depths, starting from low resistivity (<1 Ωm) near the surface down to a depth of 800 m which is followed by a fairly high resistivity (> 40 Ωm) with a thickness of about 4 km. Below it, low resistivity is found. This structure could be related to the geological stratigraphy seen in the wells. In the geological stratigraphy, the upper layers are mostly sedimentary down to a depth of 1000 m below the surface. Therefore, the low-resistivity layer close to the surface down to a depth of 800 m could be related to sedimentary deposits and formations or altered mineralizations with rock temperature of around 200-230°C. This is the smectite-zeolite zone. The higher resistivity below the low resistivity relates to the Afar Stratoid basalts. This is seen in Figure 19. At a depth of 6000 m there is low resistivity; this may be related to the main fracture zone, upflow of geothermal fluids or even the heat source.

There are resistivity variations near the surface. These variations are seen in MT soundings TDO606 and TDO807 and are probably caused by static shift. To reduce the static shift effect, transient electromagnetic (TEM) measurements are advisable, followed by joint inversion of MT and TEM data.

## ACKNOWLEDGEMENTS

I would like to thank the United Nations University Geothermal Training Programme and the Government of Iceland for giving me this opportunity to participate in this specialized training. Special gratitude goes to the former director of UNU-GTP, Dr. Ingvar B. Fridleifsson, and the new director, Mr. Lúdvík S. Georgsson, for offering me the opportunity to participate in the Geothermal Training Programme. Thanks to all staff members of UNU-GTP for their guidance and support. Special thanks to my advisors, Mr. Gylfi Páll Hersir, Mr. Knútur Árnason and Mr. Andemariam Teklesenbet, for their valuable time, special lectures, guidance and treatment. All lecturers, Orkustofnun and ISOR staff members, are greatly acknowledged for sharing their knowledge and experience. I am also grateful to the Geological Survey of Ethiopia for supporting my studies in Iceland.

Finally, I would like to thank the Almighty God for all his help.

## REFERENCES

Amdeberhan, Y., 1998: A conceptual reservoir model and production capacity estimate for the Tendaho geothermal field, Ethiopia. Report 1 in: *Geothermal training in Iceland 1998*. UNU-GTP, Iceland, UNU-GTP, 1-24.

Archie, G.E., 1942: The electrical resistivity log as an aid in determining some reservoir characteristics. *Tran. AIME, 146,* 54-67.

Árnason, K., 1989: *Central loop transient electromagnetic sounding over a horizontally layered earth*. Orkustofnun, Reykjavík, report OS-89032/JHD-06, 129 pp.

Árnason, K., 2006a: *TemX, short manual*. ISOR, Reykjavík, internal report, 17 pp.

Árnason, K., 2006b: *TEMTD (program for 1D inversion of central-loop TEM and MT data*). ISOR, Reykjavík, internal report, 16 pp.

Árnason, K., 2008: *The magnetotelluric static shift problem.* ISOR - Iceland GeoSurvey, report ÍSOR08088, 16 pp.

Castells, A.M., 2006: *A magnetotelluric investigation of geoelectrical dimensionality and study of the central Betic crustal structure*. University of Barcelona, Spain, PhD thesis, 45 pp.

Dakhnov, V.N., 1962: Geophysical well logging. *Q. Colorado Sch. Mines, 57-2*, 445 pp.

Eysteinsson, H., 1998: *TEMRESD, TEMMAP and TEMCROSS plotting programs.* ÍSOR- Iceland GeoSurvey, unpublished programs and manual.

Flóvenz, Ó.G., Spangerberg, E., Kulenkampff, J., Árnason, K., Karlsdóttir, R., Huenges, E., 2005: The role of electrical interface conduction in geothermal exploration. *Proceedings of the World Geothermal Congress 2005, Antalya, Turkey,* 9 pp.

Flóvenz, Ó.G., Hersir, G.P., Saemundsson, K., Ármannsson, H., and Fridriksson Th., 2012: Geothermal energy exploration techniques. In: Sayigh, A., (ed.), *Comprehensive renewable energy, vol. 7.* Elsevier, Oxford, 51-95.

Hersir, G.P., and Árnason K., 2009: Resistivity of rocks. *Paper presented at "Short Course on Surface Exploration for Geothermal Resources", organized by UNU-GTP and LaGeo, Santa Tecla, El Salvador*, 8 pp.

Hersir, G.P., and Björnsson, A., 1991: *Geophysical exploration for geothermal resources. Principles and applications.* UNU-GTP, Iceland, report 15, 94 pp.

Kebede, Y., 2001: Application of the resistivity method in the Krísuvík geothermal area, Reykjanes peninsula, SW-Iceland. Report 6 in: *Geothermal training in Iceland 2001*. UNU-GTP, Iceland, 115-142.

Keller, G.V., and Frischknecht, F.C., 1966: *Electrical methods in geophysical prospecting.* Pergamon Press Ltd., Oxford, 527 pp.

Lemma, Y., 2007: Magnetotelluric and transient electromagnetic methods in geothermal exploration, with an example from Tendaho geothermal field, Ethiopia. Report 11 in: *Geothermal training in Iceland 2007*. UNU-GTP, Iceland, 225-256.

Megersa, G., and Getaneh, E., 2006: *Geological surface hydrothermal alteration and geothermal mapping of Dubti-Semera area, Tendaho geothermal field*. Geological Survey of Ethiopia, unpublished report, 65 pp.

SEG, 1991: *MT/EMAP data interchange standard*. Society of Exploration Geophysicists, 112 pp.

Simpson, F., and Bahr, K., 2005: *Practical magnetotellurics*. Cambridge University Press, Cambridge, UK, 254 pp.

Teklesenbet, A., 2007: Transient electromagnetic and magnetotelluric geophysical methods in the Hengill area, SW-Iceland. Report 22 in: *Geothermal training in Iceland 2007*. UNU-GTP, Iceland, UNU-GTP, 521-554.

Teklesenbet, A., 2012*: Multidimensional inversion of MT data from Alid geothermal area, Eritrea; comparison with geological structures and identification of a geothermal reservoir*. University of Iceland, MSc thesis, UNU-GTP, Iceland, report 1, 92 pp.

Zhdanov, M.S., and Keller, G.V., 1994: *The geoelectric methods in geophysical exploration.* Elsevier, Amsterdam, 873 pp.